Title

RelB-deficient autoinflammatory pathology presents as interferonopathy, but in mice is interferon-independent.

Journal

Journal of Allergy and Clinical Immunology, 152(5)

Authors

Navarro, Héctor
Liu, Yi
Fraser, Anna
et al.

Publication Date

2023-11-01

DOI

10.1016/j.jaci.2023.06.024

Peer reviewed

HHS Public Access

Author manuscript

J Allergy Clin Immunol. Author manuscript; available in PMC 2024 February 10.

Published in final edited form as:

J Allergy Clin Immunol. 2023 November ; 152(5): 1261–1272. doi:10.1016/j.jaci.2023.06.024.

RelB-deficient autoinflammatory pathology presents as interferonopathy, but in mice is IFN-independent

Hector I. Navarro, BS[1,2], **Yi Liu, PhD**[1,2,3], **Anna Fraser, BS**[1,2,4], **Diane Lefaudeux, MEng**[1,4], **Jennifer J. Chia, MD, PhD**[1,2,5], **Linda Vong, PhD**[6], **Chaim M. Roifman, MD**[6], **Alexander Hoffmann, PhD**[1,2,4]

[1]Department of Microbiology, Immunology, and Molecular Genetics, UCLA, 611 Charles E Young Drive, Los Angeles, CA 90093

[2]Molecular Biology Institute, UCLA, 611 Charles E Young Dr E, Los Angeles, CA 90095

[3]DeepKinase Biotechnologies Ltd., 5 Kaituo Road, Haidian, Beijing, China 100085

[4]Institute for Quantitative and Computational Biosciences, Institute, UCLA, 611 Charles E Young Drive, Los Angeles, CA 90093

[5]Department of Pathology and Laboratory Medicine, UCLA, 10833 Le Conte Ave, Los Angeles, CA 90095

[6]The Canadian Centre for Primary Immunodeficiency, Immunogenomic Laboratory, Jeffrey Modell Research Laboratory for the Diagnosis of Primary Immunodeficiency, Division of Immunology/ Allergy, Department of Pediatrics, Hospital for Sick Children, and the University of Toronto, Toronto, Ontario, Canada

Abstract

Background: Autoimmune diseases are leading causes of ill health and morbidity and have diverse etiology. Two signaling pathways are key drivers of autoimmune pathology, interferon and NFκB/RelA, defining the two broad labels of interferonopathies and relopathies. Prior work established that genetic loss of function of the NFκB subunit RelB leads to autoimmune and inflammatory pathology in mice and humans.

Objective: We sought to characterize RelB-deficient autoimmunity by unbiased profiling of the stimulus-responses of immune sentinel cells, and to determine the functional role of dysregulated gene programs in the RelB-deficient pathology.

Methods: Transcriptomic profiling was performed on fibroblasts and dendritic cells derived from RelB-deficient patients and knockout mice, and transcriptomic responses and pathology were assessed in mice deficient in both RelB and the type I interferon receptor.

Corresponding Author: Alexander Hoffmann, Ph.D., Address: 570 Boyer Hall, Los Angeles, CA 90095, ahoffmann@g.ucla.edu, Phone: 310-794-9925.

Author Contributions

A.H. and H.I.N. designed and conceived the research; H.I.N., Y.L. performed experimental work; H.I.N., A.F., D.L., J.C. analyzed the data; H.I.N., C.R., A.H. discussed and interpreted results; L.V., C.R., A.H. procured samples and funding; H.I.N., A.H. wrote and Y.L., D.L., C.R. edited the manuscript.

Conflict of Interest:

The authors declare that research in this study was conducted in the absence of a conflict of interest.

Results: We found that loss of RelB in patient-derived fibroblasts and mouse myeloid cells results in elevated induction of hundreds of interferon-stimulated genes. Removing hyper-expression of the interferon stimulated gene program did not ameliorate the autoimmune pathology of RelB knockout mice. Instead, we found that RelB suppresses a different set of inflammatory response genes in a manner that is independent of interferon signaling but associated with NFκB binding motifs.

Conclusion: While transcriptomic profiling would describe RelB-deficient autoimmune disease as an interferonopathy, the genetic evidence indicates that the pathology in mice is interferon-independent.

Capsule Summary:

Loss of RelB reveals a broad interferon gene signature in patient-derived fibroblasts and mouse dendritic cells. While IFNAR deletion completely ablates this gene program, it does not diminish RelB knockout autoimmune pathology, ruling out interferonopathy.

Keywords

RelB; autoimmunity; inflammation; interferonopathy; relopathy; dendritic cells

INTRODUCTION

Autoimmune diseases (AI) and autoinflammatory (AIF) diseases are rapidly expanding categories of immune related disorders and a major health concern. Current studies estimate that there are around 150 life-long debilitating autoimmune diseases, characterized by a dysregulation of adaptive immune system, with no known cures (1) and a growing list of 40 genetically described autoinflammatory diseases, characterized by a dysregulation of the innate immune system (2). These diseases have chronic lifelong symptoms such as chronic fevers (3), arthritis (4), inflammatory bowel disease (5), hepatic and central nervous system inflammation (6,7), among other serious health issues. Our understanding of the role of chronic inflammation in other human disease such as cancer, heart disease, and psychiatric disorders is also growing rapidly (8). Therefore, understanding autoimmune and autoinflammatory diseases is critically important to therapeutically address the growing number of AI and AIF patients as well as other human diseases in which inflammation plays a key role. Autoinflammatory diseases have recently been categorized into the following five subsets based on underlying dysregulated mechanisms: inflammasomopathies, interferonopathies, unfolded protein responses/ER stress syndromes, relopathies, and uncategorized (9).

Of growing interest are interferonopathies, which are defined as diseases grouped by mendelian disorders associated with an upregulation of type I interferon (IFNs), first described in 2003 (10), and later officially categorized and termed (11). Type I IFNs are a class of antiviral, anti-inflammatory proteins first discovered in 1957 for their ability to induce influenza viral interference (12). Type I IFNs signal in a paracrine and autocrine manner via the IFN-α/β receptor (IFNAR) comprising of two subunits, IFNAR1 and IFNAR2. The IFN receptor has been shown to be expressed by virtually every nucleated

cell, of hematopoietic and non-hematopoietic origin, and while some cells are specialized producers of Type-I IFN, almost all cells are able to produce Type-I IFN (13). Upon Type I IFN binding to the IFNAR receptor, downstream transcription factor complex, ISGF3, is formed and induces the expression of interferon stimulated genes (ISGs) by binding to their promoter regions containing interferon-sensitive response elements (ISREs). Given the broad extent of the IFN-signaling network in human physiology, as one may expect, dysregulation of IFN signaling leads to a multitude of pathologies affecting various organs and organ systems. For example, USP18$^{-/-}$ mice, lacking a negative regulator of IFN-signaling, UBP43, which leads to elevated levels of conjugates to ISG15, a potently induced ISGF3 target gene, develop brain injury, accompanied by hydrocephalus and early death with 50% of mice dying at 4 weeks of age (14,15). This pathology was also seen in human patients with ISG15 null mutations, causing death or seizures in 3 patients (16). Interferonopathies can cause other harmful effects on the CNS such as epilepsy, as well as psychomotor retardation in Aicardi–Goutières syndrome (AGS) (17) and have also been shown to lead to interstitial lung disease, arthritis, panniculitis lipodystrophy, necrotizing vasculitis, bone dysplasia, and early thrombotic events among other serious symptoms (18). Importantly, while we can broadly categorize AIFs into interferonopathies, the pathological outcomes and symptoms of diseases within this category vary broadly and often have overlapping dysregulation of various immune-related signaling pathways. Many AIF diseases also share AI disease characteristics involving dysregulation in both innate and adaptive immunity. Therefore, understanding the underlying mechanisms and etiology of these pathologies in a disease-specific manner is crucial to effectively tailor therapeutic approaches for patients with highly unique genetic lesions.

Recently, pediatric patients with a homozygous null mutation in the gene encoding NFκB subunit, RelB, were described (19–21). These patients presented a combined immunodeficiency phenotype with failure to thrive and a significantly impaired ability to produce specific antibodies *in vivo* (20). Interestingly, these patients were also characterized with an autoimmune pathology presenting severe autoimmune skin disease and rheumatoid arthritis involving altered thymic T cell maturation with reduced output and production of a skewed T-cell repertoire with expansion of clones (21). While defects in the adaptive immune system were found and well described in these studies, the description of the patient innate immune function was more limited but appeared to behave normally relative to adaptive immune system, as measured by TNF secretion in patient derived monocytes. However, patient derived fibroblasts, key pathogen sensing sentinel cells, revealed to have elevated TNF-induced RelA DNA binding activity (21).

Findings in the RelB-null human pathology strikingly resembled previously reported phenotypes of *RelB*$^{-/-}$ mice (multi-organ inflammation, thymic atrophy, reduction of thymocytes, impaired cell mediated immune response, but normal T and B cell development (22), suggesting a conserved mechanisms between human and mouse pathology. In mice, functional adoptive transfer studies identified dendritic cells (DCs), key pathogen-sensing immune sentinel cells, to be key drivers of the lung inflammatory pathology seen in *RelB*$^{-/-}$ mice (23). Another study supported these findings by demonstrating a restoration of the thymic atrophy and the numbers of thymic Foxp3+ T-regs in *RelB*$^{-/-}$ mice upon adoptive transfer of *RelB*$^{+}$ DCs (24). However, subsequent studies that addressed the auto-

inflammatory mechanisms that causes immune sentinel cells to drive the pathology have reported several different mechanisms and no consensus has emerged (25–27).

We aimed to further understand the mechanistic dysregulation of RelB-null immune sentinel cells as they contribute to *RelB*$^{-/-}$ auto-inflammatory disease. Given recent reports of elevated IFN signaling caused by RelB-deficiency (28–30), we hypothesized dysregulation of the IFN pathway may be present in RelB-null patient derived sentinel cells, potentially implying immediate clinically relevant characterization of the RelB null pathology as an interferonopathy. Indeed, we found that loss of RelB in patient-derived fibroblasts and mouse DCs, but not macrophages, results in elevated expression of interferon-stimulated genes (ISGs) that is dependent on elevated type I IFN signaling. However, to our surprise, while the hyper-expression of ISGs is a prominent aspect of the loss of RelB phenotype, complete ablation of type I IFN signaling in the mouse did not ameliorate the RelB pathology. We found instead that RelB directly suppresses a myriad of IFN-independent pro-inflammatory and immune response genes which promote a cell-intrinsic hyper-activated inflammatory state both in *RelB*$^{-/-}$ human fibroblasts and mouse DCs, which in turn are likely key contributors to the RelB-null autoimmune and autoinflammatory pathology.

Methods

Patient-Derived Fibroblasts

Total RNA was prepared as described (31). Strand-specific libraries were generated from 200 ng total RNA using the KAPA Stranded mRNA sequencing and Library Preparation Kit (Illumina). cDNA libraries were single-end sequenced (50bp) on an Illumina HiSeq 2000. RNA-seq reads were trimmed using cutadapt v1.12 (31) to remove low quality ends as well as removing remaining adapter sequence. Then reads were aligned on the human genome (hg38) using STAR software v2.5.2b (32). Aligned reads were filtered using samtools v1.3.1 (33) to keep only uniquely aligned reads. Gene expression quantification was done using featureCounts v1.5.1 (34) software and GENCODE v23 gene annotation (35). Differential expressed genes were selected using edgeR (36) with a 4 fold and 0.01 FDR threshold in either WT or patient samples.

Clustering of differentially expressed genes was done using a kmean method to identify clusters of DEG with similar dynamic profiles. Gene ontology and motif analysis was done via homer suite considering regulatory regions within −4kb to 1kb from the transcription start site.

Mice and bone marrow-derived dendritic cells

Wild-type and transgenic mice were housed in pathogen-free conditions at University of California, Los Angeles. *RelB*$^{-/-}$ mice were generated by breeding *RelB*$^{+/-}$ mice and *IFNAR*$^{-/-}$*RelB*$^{-/-}$mice were generated by mating *IFNAR*$^{-/-}$*RelB*$^{+/-}$ *or IFNAR*$^{+/-}$*RelB*$^{+/-}$ mice to each other. All mice used for RNA-seq experiments were between 6 to 12 weeks at day of experiment, both male and female mice were used for experiments. Bone marrow cells were isolated from mouse femurs and cultured with M-CSF-containing L929-conditioned medium for BMDMs or with 20 ng/ml GM-CSF and 10 ng/ml IL-4 to

produce BMDCs with half the media being replaced on day 3 and 6 as previously reported (37). Cells were stimulated with CpG (0.1μM) (Invivogen ODN 1668 Cat# tlrl-1668), or Poly(I:C) HMW (10μg/mL) (Invivogen Cat#tlrl-pic) and collected at specified timepoints in Invitrogen™ TRIzol™ Reagent (Cat# 15–596-018), RNA was extracted using Qiagen RNeasy Mini Kit (Cat #74106) as described (39).

Transcriptome profiling

RNA was used for Illumina bead Arrays as described (31) and for RNA-seq as described (40). Briefly, libraries were prepped using KAPA Stranded mRNA-Seq Kit Illumina® platform KR0960 – v3.15 using 1μg of RNA per sample measured using Qubit 2.0 fluorometer. Final libraries were checked via agarose gel and multiplexed with a maximum of 24 samples per sequencing reaction. Libraries were sequenced using Illumina HiSeq 3000 with single end 50bp reads at the UCLA Technology Center for Genomics & Bioinformatics.

Bioinformatic Analysis

Reads were trimmed using cutadapt (31) (cutoff q=20) and mapped to the mm10 genome. Processed reads showed high quality reads and alignment scores. The October 2014 version of the Ensembl database was used to extract gene annotation information. CPM values were generated using edgeR (36) to normalize the raw counts data based on sequencing depth. To permit fold change calculations, a pseudocount of 1 CPM was added. Induced genes were selected using a $\log_2$FC>1 cutoff for any stimulated timepoint relative to 0hr unstimulated control, transcripts with empty gene names were removed. Data was z-scored and plotted using the pheatmap R package. Fold differences of genes within heatmaps was calculated by first calculating the fold differences for all individual genes between genotype of interest and WT or *IFNAR*$^{-/-}$ control CPM (Genotype X)/CPM (Genotype Y) for each individual time point. Average fold differences were then calculated by averaging the fold differences of all genes within each cluster for each individual time point. Gene ontology and motif analysis was done via homer suite considering regulatory regions within −1kb to 1kb from the transcription start site. Line graphs of individual genes were generated using GraphPad Prism.

Tissue Isolation and Fixation

Spleens were isolated from age matched mice immediately after euthanizing and subsequently rinsed with PBS. Excess PBS was removed from spleens and were subsequently weighed. Fixation was done in 10% Formaldehyde for 46–48hrs. Tissue was processed, sectioned, and hematoxylin and eosin stained by the UCLA Translational Pathology Core Laboratory (TPCL).

REB approval

All patient studies were approved by the SickKids Research Ethics Board (Protocol no. 1000005598).

RESULTS

Fibroblasts obtained from a human RelB-null donor show hyperexpression of type I interferon and interferon-stimulated genes.

To characterize the transcriptome-wide defects caused by the loss of RelB, we performed an unbiased differential gene expression analysis using fibroblasts obtained from a previously reported combined immunodeficiency patient (P1) with an AI disease pathology arising as a consequence from a rare homozygous mutation in the *RelB* gene resulting in the complete loss of RelB protein, and their healthy close relative with homozygous copies of WT *RelB* (Control) [20,21]. To experimentally model immune stimulation *via* pattern recognition receptors (PRRs) that may occur in response to pathogen exposure or tissue injury, we stimulated fibroblasts with TLR3 agonist poly(I:C) (10μg/mL) in replicate. After collecting RNA at 5 time points (0, 2, 4, 8, 15 h) we performed whole transcriptome RNA-seq and bioinformatically identified 740 genes that were induced with a FC>4 and FDR <0.01 threshold in either WT or P1 replicate samples. Applying k-means clustering to the expression data of these genes, we identified 6 distinct clusters of differentially expressed genes that were hyper-expressed in P1 (Fig. 1a). A small proportion of genes clustered within cluster A (33 genes) and cluster B (63 genes) but resulted in weak or no motif enrichment results, however most genes clustered in hyper-expressed clusters C through F, which revealed to have average fold differences in counts per million (CPM) ranging from 1.6x and 14x between P1 and control fibroblasts at any of the measured timepoints (Fig. 1a, Supplementary Table 1). To identify potential regulatory features of these genes we performed motif enrichment analysis that considered −4kb to +1kB with respect to the transcription start site (TSS) of the regulatory region of each gene. Genes within hyper-expressed clusters C (102 genes) and D (175 genes) were statistically enriched for NFκB motifs in regulatory regions, while hyper-expressed clusters E (210 genes) and F (157 genes) were statistically enriched for IRF and ISRE motifs (Fig. 1b). This analysis suggested two major categories of dysregulated genes: IFN-stimulated genes (ISGs) and NFκB-regulated genes. To identify potential biological functions, we performed gene ontology (GO) analysis. Clusters C and D were associated with terms invoking NFκB activating pathways such as “TNF” and “LPS signaling”. Clusters E and F were associated with terms invoking IFN-inducing pathways including Type I “interferon-α” and Type II “interferon-γ response” (Fig. 1c). Analysis of individual genes within clusters E and F revealed many hyper-expressed ISGs including *Oasl*, *Oas2*, *Ifit1, Ifit2*, *Mx2,* and *Isg20* (Fig. 1d). Given that ISGs may be activated by Type I, II, and III IFNs (41), we evaluated the expression of IFN family members. We found *Ifnb1* and *Ifnl3* to be hyper-expressed in fibroblasts derived from P1 (Fig. 1d). Together, these data establish that loss of function of RelB results in hyper-induction of not only NFκB-associated genes but a large ISG expression program prompting the question of whether it drives the described autoimmune/autoinflammatory pathology.

Loss of RelB in mouse myeloid cells recapitulate hyperexpression of type I IFN and interferon stimulated gene programs observed in patient fibroblasts.

Adoptive transfer studies suggested that myeloid cells (MCs) play a key role in driving the lethal multi-organ inflammation in $RelB^{-/-}$ mice (23,24). We therefore undertook

transcriptomic profiling of mouse MCs produced by differentiating wild-type and *RelB*$^{-/-}$ bone marrow cells with GMCSF + IL-4 or MCSF, which generate primarily dendritic cells or macrophages, respectively (38,42). We then stimulated these cells with TLR3 or TLR9 agonists poly(I:C) (10μg/mL) - or CpG (0.1μM) over a 24-hour time course and performed unbiased differential gene expression analyses followed by k-means clustering. Our analysis of GMCSF MCs revealed 425 and 415 genes induced (logFC>1) with poly(I:C) and CpG respectively. Differential gene expression analysis revealed clusters of genes which were hyper-expressed both in a basal state and upon poly(I:C)- or CPG- stimulation (Fig. 2a and 2b). Poly(I:C)-stimulated genes in hyper-expressed cluster A (72 genes) showed average fold differences in expression ranging from 1.5x to 3.9x between *RelB*$^{-/-}$ and WT GMCSF MCs at any of the measured time points (Fig. 2a, Supplementary Table 2). Likewise, CpG stimulated genes in hyper-expressed cluster C (116 genes) showed average fold differences in expression ranging from 1.2x to 2.5x between *RelB*$^{-/-}$ and WT GMCSF MCs at any of the measured time points (Fig. 2c, Supplementary Table 2), and shared 55 out of the 72 genes with poly(I:C) hyper-expressed cluster A. Motif enrichment analysis of hyper-expressed cluster A in poly(I:C)-stimulated GMCSF MCs revealed the ISRE as the top motif in a statistical enrichment analysis that considered −1kb to +1kB with respect to the TSS of the regulatory region of each gene (Fig. 2a, bottom). Similarly, in CpG-stimulated GMCSF MCs, hyper-expressed cluster C also yielded the ISRE as the top statistically enriched motif (Fig. 2c, bottom). Furthermore, GO analysis of these clusters revealed ISG-inducing pathways, “IFN-α response”, and “IFN-γ response” among the top terms for both clusters. These data suggested that hyper-expressed genes in these clusters are ISGs, perhaps elevated by hyper-induction of IFNs in *RelB*$^{-/-}$ GMCSF MCs. We therefore analyzed a set of IFN genes and found *Ifnb1* to be elevated, with concurrent hyper-expression of ISGs, *Oasl*, *Oas1, Oas2*, *Ifit2*, and *Ifit3*, in both poly(I:C)- and CPG-stimulated conditions (Fig. 2c and 2d). Like poly(I:C)-stimulated RelB-null patient-derived fibroblasts, *RelB*$^{-/-}$ GMCSF MCs stimulated with poly(I:C) also revealed a gene cluster (cluster B) which was hyper-expressed at the late 24h stimulated timepoint with an average expression fold difference of 1.45x between *RelB*$^{-/-}$ and WT GMCSF MCs. This cluster yielded NFκB as the top result in motif enrichment analysis. All other clusters in both poly (I:C) and CpG were unchanged, containing average expression fold differences ranging from .9x to 1.17x between *RelB*$^{-/-}$ and WT GMCSF MCs at all time points (Fig. 2a and 2c, Supplementary Table 2). Next, we asked whether myeloid cells differentiated with M-CSF (MCSF MCs) showed similar transcriptomic dysregulation as GMCSF MCs. We generated MCSF MCs from *RelB*$^{-/-}$ and WT control bone marrow and undertook an analogous analysis following stimulation. We identified 1,243 unique induced genes (logFC>1) with LPS and performed differential gene expression analysis. In contrast to our findings with GMCSF MCs, our analysis of MCSF MCs revealed no differentially expressed gene clusters between WT and *RelB*$^{-/-}$ genotypes, with all clusters revealing average expression fold differences ranging from .9x to 1.1x between *RelB*$^{-/-}$ and WT MCSF MCs at all time points. (Fig. 2e, Supplementary Table 2). The lack of expression phenotype may be because MCSF MCs show lower levels of *RelB* expression compared to GMCSF MCs (39). Together, these results indicated that the loss of RelB results in a cell-specific transcriptome phenotype, with PAMP-stimulated GMCSF MCs showing broad and pronounced dysregulation of interferons and interferon-stimulated genes. Given the physiological importance of dendritic cells in both innate immunity as

cytokine and chemokine producers (43), and adaptive immunity as antigen-presenting cells (44,45) and, in addition their demonstrated involvement in the *RelB*$^{-/-}$ autoinflammatory pathology (23,24), we proceeded with *RelB*$^{-/-}$ GMCSF MCs as a model system for further studies.

Compound deficiency of the type I interferon receptor ablates the hyperactivation of the interferon-stimulated gene program in RelB-deficient dendritic cells.

While the expression of ISGs is primarily driven by the transcription factor complex ISGF3 or STAT1 homodimers (GAF) which are downstream of IFN signaling (46), many ISGs also contain NFκB motifs and have been shown to be regulated by NFκB (47–49). However, the potential role of NFκB RelB in regulating ISGs or other immune response genes remains largely unknown. Given the hyper-expression of IFNβ, it remained unclear whether hyperexpression of ISGs is caused by elevated IFNβ signaling and secondary ISGF3 activation, or by IFN-independent regulatory mechanisms more directly caused by the loss of RelB. To distinguish between these two mechanisms, we generated an *IFNAR*$^{-/-}$*RelB*$^{-/-}$ double mutant mouse which results in complete ablation of IFNβ signaling and thus a loss of secondary IFN-dependent gene expression programs, while IFN-independent gene expression remains. Using bone marrow from double *IFNAR*$^{-/-}$*RelB*$^{-/-}$, single *IFNAR*$^{-/-}$, single *RelB*$^{-/-}$, and WT mice, we produced GMCSF MCs and performed RNA-seq followed by differential gene expression analysis and k-means clustering.

To distinguish between dysregulated responses that were interferon-dependent or independent, we aimed to identify clusters with hyper-expressed genes shared between *RelB*$^{-/-}$ and *IFNAR*$^{-/-}$*RelB*$^{-/-}$ GMCSF MCs and that were not hyper-expressed in single *IFNAR*$^{-/-}$ cells. We therefore first identified 1,123 induced (logFC>1) genes upon CpG (0.1μM) stimulation in WT or *RelB*$^{-/-}$ MCs, and further filtered for genes that were hyper-expressed (FC>1.5) in *RelB*$^{-/-}$ MCs relative to WT MCs. We identified 334 genes which met these criteria and then examined their expression patterns in *IFNAR*$^{-/-}$ and *IFNAR*$^{-/-}$*RelB*$^{-/-}$ MCs. Using k-means clustering on these genes of interest, our analysis identified hyper-expressed cluster A (215) which had average fold differences ranging from 1.8x to 2.1x between *IFNAR*$^{-/-}$*RelB*$^{-/-}$ MCs relative to WT MCs and 1.4x to 1.6x relative to single *IFNAR*$^{-/-}$MCs at all observed timepoints (Fig. 3a, Supplementary Table 3), suggesting these may be genes directly affected by the loss of RelB, and independently of IFN signaling. On the other hand, the induction of genes in hyper-expressed cluster B (119 genes) was lost in both *IFNAR*$^{-/-}$*RelB*$^{-/-}$ and single *IFNAR*$^{-/-}$MCs, having average CPM fold changes differences of .6x in both *IFNAR*$^{-/-}$*RelB*$^{-/-}$ and *IFNAR*$^{-/-}$ MCs relative to WT MCs at the late 8h stimulated timepoint. These data suggested that genes in this cluster are ISGs and are hyper-expressed in *RelB*$^{-/-}$ due to elevated IFNβ signaling. Motif enrichment analysis (-1kb to +1kB from the TSS) of cluster A genes hyper-expressed specifically in *RelB*$^{-/-}$ and *IFNAR*$^{-/-}$*RelB*$^{-/-}$mutants revealed NFκB as the top statistically enriched motif and GO analysis revealed NFκB-inducing pathways “CD40”, “TNF”, and “LPS-signaling” as the top terms (Fig. 3b). As expected, motif enrichment analysis of IFN-dependent cluster B revealed ISRE as the top statistically enriched motif and GO analysis resulted in ISG-inducing pathways, “IFN-λ” and “IFN-β”, as the top terms (Fig. 3b). Our analysis of poly(I:C) (10ug/mL) stimulated MCs also yielded an IFN-dependent

and independent cluster (Supplementary Fig. S1), with the IFN-dependent cluster sharing 44 out of 82 genes with the CpG IFN-dependent cluster, and the and the IFN-independent clusters sharing 58 out of 130 genes. (Supplementary Table 3, Supplementary Table 4).

These data suggested that while there are ISGs that are indirectly hyper-expressed by the loss of RelB, genes directly dysregulated by the loss of RelB are primarily NFκB-regulated immune response genes. Analysis of individual genes within the IFN-independent cluster A and genes with similar IFN-independent expression patterns revealed a myriad of NFκB-regulated pro-inflammatory genes including inflammatory chemokines, *Ccl5* and *Ccl22,* co-stimulatory molecules *Cd80 and Cd86*, canonical and non-canonical NFκB stimulating receptor *Cd40.* As well as IFN signaling activators and p-IRF3 kinases, *Map3k14* (NIK), and *Ikbke* (IKKε) (50,51) (Fig. 3c). We found these genes were also hyper-expressed in *IFNAR*$^{-/-}$*RelB*$^{-/-}$ MCs upon poly (I:C) stimulation (Supplementary Fig. S2). We then asked if these genes may also be hyper-expressed in RelB-null patient samples and we found 51 out of 334 of these genes were hyper-expressed in human RelB-null fibroblast from P1 (Fig. 3d). Together, these data suggest that while the ISG transcriptome signature is a substantial portion of the hyperexpression in RelB-null immune sentinel cells, RelB-loss also results in hyperexpression of many immune response genes *via* IFN-independent mechanisms.

Ablation of the elevated type I IFN stimulated gene program does not rescue RelB-null pathology.

Having established that a significant proportion of the hyper-expressed genes associated with RelB-loss are due to elevated IFN signaling, we asked whether these genes cause or contribute to the inflammatory pathology described for the *RelB*$^{-/-}$ mouse. To answer this, we examined the health state of *RelB*$^{-/-}$, and *IFNAR*$^{-/-}$*RelB*$^{-/-}$ double mutant mice, as well as controls. Upon phenotypical analysis, the 4-week old *IFNAR*$^{-/-}$*RelB*$^{-/-}$ mouse appeared runted, much smaller than its healthy heterozygous littermate, and similar to *RelB*$^{-/-}$ mice (22) (Fig. 4a). *IFNAR*$^{-/-}$*RelB*$^{-/-}$ mice were found to have marked splenomegaly similar to *RelB*$^{-/-}$ mice (22) (Fig. 4b). The spleen from *IFNAR*$^{-/-}$*RelB*$^{-/-}$ weighed 2.9x and 2.5x more than spleens from WT and single *IFNAR*$^{-/-}$ mice respectively (Fig. 4c). Additionally, histological analysis of *IFNAR*$^{-/-}$*RelB*$^{-/-}$ -spleens revealed marked red pulp expansion and a reduction in white pulp, similar to both our observations and prior reported findings in the *RelB*$^{-/-}$ mice (22) (Fig. 4d). Upon assessment of serum cytokine levels, *RelB*$^{-/-}$ mice revealed elevated levels of CXCL10 and IL-6 (p=.051), consistent with previous reports in the skin and lungs of *RelB*$^{-/-}$ mice, respectively (23,52). However, the levels of these elevated cytokines in the serum were not diminished by *IFNAR* deletion (Fig. S3). These data together identify two unique classes of genes regulated by NFκB subunit RelB in immune sentinel cells relevant to human pathology, IFN-dependent ISGs, and IFN-independent inflammatory genes. Most importantly these data determine clinically relevant findings in understanding which genes play critical roles in loss of RelB autoinflammatory pathology. While we have shown that the loss of RelB indirectly regulates ISGs via Type I IFN signaling, these genes seem to play a superfluous role in critical aspects of the multi-organ inflammation seen in *RelB*$^{-/-}$ mice, instead RelB directly suppresses IFN-independent genes that are likely the critical drivers of inflammation by immune sentinel cells. These

data inform future studies for clinical targets in treating loss of RelB and other autoimmune and autoinflammatory disorders.

DISCUSSION

Here we report a molecular characterization of auto-inflammatory disease caused by RelB-deficiency. Taking an unbiased approach via transcriptome analysis, we found fibroblasts derived from RelB-deficient patients showed hyper-expression of IFN-β and interferon-stimulated genes (ISGs) when exposed to the PRR agonist poly(I:C). This was also seen in mouse DCs (Fig. 2a) and found to be dependent on signaling via the type I interferon receptor, IFNAR (Fig. 1a, 3a). Initially, we expected to provide evidence to categorize the *RelB*$^{-/-}$ null pathology as an interferonopathy-driven AIF disease, thereby providing a clinically relevant therapeutic target to ameliorate the auto-inflammatory pathology. However, we found that compound knockout *IFNAR*$^{-/-}$*RelB*$^{-/-}$ mice showed no amelioration of critical aspects of the auto-inflammatory disease characteristic of RelB-deficient mice. Compound knockouts remained drastically runted, presented hunched backs, and had enlarged abdomens, like *RelB*$^{-/-}$ mice (22). Additionally, no improvement in the organ inflammation was seen as measured by splenomegaly or histological analysis of red and white pulp.

Given the pronounced ISG expression signature in RelB-deficient human fibroblasts and murine dendritic cells, this is a surprising result. We wondered whether the compound mutant might have residual ISG expression via STAT1 or IRF3-dependent compensatory mechanisms (53,54), but detailed analysis confirmed that ISG expression was diminished to baseline or below by the *IFNAR* knockout mutation (Fig. 4e). Thus, the pathology in C57/Bl6 mice resulting from RelB-deficiency, despite being associated with a pronounced interferon signature, is not an interferonopathy. However, given that our studies were done with a specific congenic mouse strain, under pathogen-free conditions, we cannot rule out type I IFN involvement in RelB knockout pathologies in other genetic backgrounds or in the context of diverse microbial exposure, which may be relevant to human pathology (55). Additionally, we cannot rule out the potential role of other classes of interferons given that our approach was restricted to deletion of type I interferon signaling.

What may be causing or contributing to the pathology if elevated ISGs are not? We focused our attention to IFN-independent genes that remain elevated when *IFNAR* is also knocked out. We identified a group of pro-inflammatory genes that were elevated in RelB-null patient-derived fibroblasts, as well as in murine *RelB*$^{-/-}$ DCs. Importantly, this gene cluster remained elevated in DC derived from *IFNAR*$^{-/-}$*RelB*$^{-/-}$ mice. Our analysis of this cluster of dysregulated genes revealed the NFκB motif as the top motif enriched near the regulatory regions of these genes. Interestingly, in fibroblasts from patients in a different family in which *RelB* expression is reduced but not absent, a cluster of hyper-induced genes also showed enrichment of the NFκB motif (19). This supports the notion that RelB-deficiency leads to a pathology that can be categorized as a relopathy.

Among these dysregulated genes associated with the RelB relopathy are potent pro-inflammatory chemokines, Ccl5 and Ccl22. Ccl5 is a potent regulator of inflammation and

chemotaxis and is of great therapeutic interest in diseases involving immune dysregulation such as inflammatory bowel disease, atherosclerosis, hepatic inflammation, and many cancers (56), importantly Ccl5 is a potent recruiter of T cells into sites of inflammation and can also recruit macrophages, eosinophils, and basophils (57). Given that MCs reside in all peripheral tissues (58) and fibroblasts are found in most tissues of the body (59), Ccl5 hyper-expressing fibroblasts and GMCSF MCs in *RelB*$^{-/-}$ mice and human patients may explain the initial recruitment of lymphocytes into inflamed organ tissues. MCs are also professional antigen presenting cells responsible for initiating antigen-specific T-cell immunity. T-cells require a secondary co-stimulation signal after TCR binding to become active, of which CD80, CD86, and CD40 are key co-stimulatory signaling molecules (60,61). The hyper-expression of CD80, CD86, and CD40 in *IFNAR*$^{-/-}$*RelB*$^{-/-}$ GMCSF MCs, suggests that these cells may exist in an intrinsic auto-inflammatory state that may hyper-activate T-cell mediated immune response at sites of inflammation in *RelB*$^{-/-}$ mice. This is consistent with findings in RelB-null human patients of high peripheral T cell numbers with clonally expanded populations as shown by TCR-Vb analysis (20,21), along with previous reports demonstrating that the multiorgan inflammation, myeloid hyperplasia, and inflammatory skin lesions are T-cell dependent mechanisms in *RelB*$^{-/-}$ mice (52,62). In addition, the cluster of IFN-independent *RelB*$^{-/-}$ dysregulated genes included *Ikbke*, as well as non-canonical NFκB activator Map3k14, which are both established Type I IFN inducers (51,63), prompting the question of whether these may contribute to the onset of IFN dysregulation. However, since our data indicate that the ISG expression program is not contributing to the auto-inflammatory pathology, this question was not further pursued.

In clinical settings, hyper-expression of ISGs, a hallmark of interferonopathies, has been associated with hepatosplenomegaly, meningoencephalitis, interstitial lung disease, recurrent unexplained fever, inflammatory organ damage, high mortality, and autoimmune characteristics (18,64,65), some of which are symptoms seen in the *RelB*$^{-/-}$ pathology. Clinical diagnosis of interferonopathies relies on an “interferon score” by measuring the expression of a panel of interferon-stimulated genes (66), a type-I IFN-response-gene score (IRG-S), cytokine profiling, clinical phenotyping, or next-generation sequencing (NGS) (18). Testing therapeutic targets along the IFN-axis in many human trials showed moderate success with monoclonal antibodies against IFNAR in treating systemic lupus erythematosus (SLE) (67), a well characterized interferonopathy (68). However, patient response rates remained below 50%, and many other clinical anti-IFN trials have produced mixed results (64). In the mouse, lupus models have a higher level of success with anti-IFNAR antibody therapy extending survival from ~20% in controls to ~70% with treatment (69), raising the question of what may account for the large variation in response to anti-interferon therapy.

Interestingly, in multiple studies SLE patients have also been characterized with A20 haplo-insufficiency (HA20), an autoinflammatory relopathy, presenting with systemic inflammation and increased NFκB-mediated pro-inflammatory cytokines (70,71), however these studies did not test for an IFN-signature. A separate study characterizing 30 patients with mutations in the, *TNFAIP3* gene (encoding A20), and 8 other clinically diagnosed HA20 patients showed that many of these patients were previously diagnosed with diseases associated with interferonopathies and other inflammatory mechanisms such as SLE, autoimmune hepatitis, and juvenile idiopathic arthritis (72–74).

Our studies presented here and by Roifman et al. (19) indicate that in RelB-deficient autoimmunity a presentation of interferonopathy is secondary to relopathy-type auto-inflammatory mechanisms, establishing a hierarchical relationship. While prior molecular characterization of human monogenic or polygenic pathologies suggests similarities to RelB-deficiency in the presentation of the pathology, it remains unclear whether the described molecular mechanisms and hierarchy apply. Yet, these findings may provide a potential explanation for the lack of efficacy in interferonopathy patients to therapeutics that target the IFN-axis (75). In sum, our findings emphasize that a presentation of interferonopathy does not necessarily render the interferon pathway an effective drug target and underscores the need for continued characterization of NFκB-driven auto-inflammatory mechanisms to develop effective therapies for relopathies.

Supplementary Material

Refer to Web version on PubMed Central for supplementary material.

Acknowledgments

We acknowledge support of a National Science Foundation Graduate Research Fellowship DGE-1540604 & DGE-2034835 (HIN), and a QCB Collaboratory fellowship (DL), and research funds from NIH R21AI128646 (AH). We acknowledge the UCLA Technology Center for Genomics & Bioinformatics and the Translational Pathology Core Laboratory (TPCL).

Funding:

This work was supported by a National Science Foundation Graduate Research Fellowship DGE-1540604 & DGE-2034835 (HIN), and a QCB Collaboratory fellowship (DL), and research funds from NIH R21AI128646 (AH).

Data Availability Statement

The experimental data is available on the Gene Expression Omnibus: GSE224515 and is available in the supplemental data.

Abbreviations:

AGS	Aicardi–Goutières syndrome
AI	autoimmune
AIF	autoinflammatory
CPM	counts per million
DC	dendritic cell
GO	gene ontology
HA20	A20 haplo-insufficiency
IFN	interferon
IFNAR	IFN-α/b receptor

ISG	interferon stimulated genes
ISRE	interferon sensitive response elements
MC	myeloid cell
PRR	pattern recognition receptor
SLE	systemic lupus erythematosus
TSS	transcription start site

References

1. Committee for the Assessment of NIH Research on Autoimmune Diseases, Board on Population Health and Public Health Practice, Health and Medicine Division, National Academies of Sciences, Engineering, and Medicine. Enhancing NIH Research on Autoimmune Disease [Internet] Washington (DC): National Academies Press (US); 2022 [cited 2022 Nov 2]. (The National Academies Collection: Reports funded by National Institutes of Health). Available from: http://www.ncbi.nlm.nih.gov/books/NBK580299/
2. Savic S, Coe J, Laws P. Autoinflammation: Interferonopathies and Other Autoinflammatory Diseases. J Invest Dermatol 2022 Mar;142(3 Pt B):781–92. [PubMed: 34887082]
3. Ancient missense mutations in a new member of the RoRet gene family are likely to cause familial Mediterranean fever. The International FMF Consortium - PubMed [Internet] [cited 2022 Nov 2]. Available from: https://pubmed.ncbi.nlm.nih.gov/9288758/
4. Shoham NG, Centola M, Mansfield E, Hull KM, Wood G, Wise CA, et al. Pyrin binds the PSTPIP1/CD2BP1 protein, defining familial Mediterranean fever and PAPA syndrome as disorders in the same pathway. Proc Natl Acad Sci U S A 2003 Nov 11;100(23):13501–6. [PubMed: 14595024]
5. Romberg N, Al Moussawi K, Nelson-Williams C, Stiegler AL, Loring E, Choi M, et al. Mutation of NLRC4 causes a syndrome of enterocolitis and autoinflammation. Nat Genet 2014 Oct;46(10):1135–9. [PubMed: 25217960]
6. Lam MT, Coppola S, Krumbach OHF, Prencipe G, Insalaco A, Cifaldi C, et al. A novel disorder involving dyshematopoiesis, inflammation, and HLH due to aberrant CDC42 function. J Exp Med 2019 Oct 10;216(12):2778–99. [PubMed: 31601675]
7. Gavazzi F, Cross ZM, Woidill S, McMann JM, Rand EB, Takanohashi A, et al. Hepatic Involvement in Aicardi-Goutières Syndrome. Neuropediatrics 2021 Dec;52(6):441–7. [PubMed: 33445189]
8. Arakelyan A, Nersisyan L, Poghosyan D, Khondkaryan L, Hakobyan A, Löffler-Wirth H, et al. Autoimmunity and autoinflammation: A systems view on signaling pathway dysregulation profiles. PLoS ONE 2017 Nov 3;12(11):e0187572. [PubMed: 29099860]
9. Rood JE, Behrens EM. Inherited Autoinflammatory Syndromes. Annu Rev Pathol Mech Dis 2022;17(1):227–49.
10. Crow YJ, Black DN, Ali M, Bond J, Jackson AP, Lefson M, et al. Cree encephalitis is allelic with Aicardi-Goutiéres syndrome: implications for the pathogenesis of disorders of interferon alpha metabolism. J Med Genet 2003 Mar 1;40(3):183–7. [PubMed: 12624136]
11. Crow YJ. Type I interferonopathies: a novel set of inborn errors of immunity. Ann N Y Acad Sci 2011;1238(1):91–8. [PubMed: 22129056]
12. Isaacs A, Lindenmann J. Virus interference. I. The interferon. Proc R Soc Lond B Biol Sci 1957 Sep 12;147(927):258–67. [PubMed: 13465720]
13. Ali S, Mann-Nüttel R, Schulze A, Richter L, Alferink J, Scheu S. Sources of Type I Interferons in Infectious Immunity: Plasmacytoid Dendritic Cells Not Always in the Driver's Seat. Front Immunol [Internet] 2019 [cited 2022 Nov 2];10. Available from: https://www.frontiersin.org/articles/10.3389/fimmu.2019.00778

14. Knobeloch KP, Utermöhlen O, Kisser A, Prinz M, Horak I. Reexamination of the Role of Ubiquitin-Like Modifier ISG15 in the Phenotype of UBP43-Deficient Mice. Mol Cell Biol 2005 Dec 15;25(24):11030–4. [PubMed: 16314524]
15. Ritchie KJ, Malakhov MP, Hetherington CJ, Zhou L, Little MT, Malakhova OA, et al. Dysregulation of protein modification by ISG15 results in brain cell injury. Genes Dev 2002 Sep 1;16(17):2207–12. [PubMed: 12208842]
16. Zhang X, Bogunovic D, Payelle-Brogard B, Francois-Newton V, Speer SD, Yuan C, et al. Human intracellular ISG15 prevents interferon-α/β over-amplification and auto-inflammation. Nature 2015 Jan;517(7532):89–93. [PubMed: 25307056]
17. Crow YJ, Zaki MS, Abdel-Hamid MS, Abdel-Salam G, Boespflug-Tanguy O, Cordeiro NJV, et al. Mutations in ADAR1, IFIH1, and RNASEH2B Presenting As Spastic Paraplegia. Neuropediatrics 2014 Dec;45(06):386–91. [PubMed: 25243380]
18. d'Angelo DM, Di Filippo P, Breda L, Chiarelli F. Type I Interferonopathies in Children: An Overview. Front Pediatr 2021 Mar 31;9:631329. [PubMed: 33869112]
19. Sharfe N, Dalal I, Naghdi Z, Lefaudeux D, Vong L, Dadi H, et al. NFκB pathway dysregulation due to reduced RelB expression leads to severe autoimmune disorders and declining immunity. J Autoimmun 2022 Nov 17;102946. [PubMed: 36402602]
20. Merico D, Sharfe N, Hu P, Herbrick JA, Roifman CM. RelB deficiency causes combined immunodeficiency. LymphoSign J 2015 Sep;2(3):147–55.
21. Sharfe N, Merico D, Karanxha A, Macdonald C, Dadi H, Ngan B, et al. The effects of RelB deficiency on lymphocyte development and function. J Autoimmun 2015 Dec 1;65:90–100. [PubMed: 26385063]
22. Weih F, Carrasco D, Durham SK, Barton DS, Rizzo CA, Ryseck RP, et al. Multiorgan inflammation and hematopoietic abnormalities in mice with a targeted disruption of RelB, a member of the NF-κB/Rel family. Cell 1995 Jan 27;80(2):331–40. [PubMed: 7834753]
23. Nair PM, Starkey MR, Haw TJ, Ruscher R, Liu G, Maradana MR, et al. RelB-Deficient Dendritic Cells Promote the Development of Spontaneous Allergic Airway Inflammation. Am J Respir Cell Mol Biol 2018 Mar;58(3):352–65. [PubMed: 28960101]
24. O'Sullivan BJ, Yekollu S, Ruscher R, Mehdi AM, Maradana MR, Chidgey AP, et al. Autoimmune-Mediated Thymic Atrophy Is Accelerated but Reversible in RelB-Deficient Mice. Front Immunol 2018;9:1092. [PubMed: 29872433]
25. Liu Y, Wang X, Yang F, Zheng Y, Ye T, Yang L. Immunomodulatory Role and Therapeutic Potential of Non-Coding RNAs Mediated by Dendritic Cells in Autoimmune and Immune Tolerance-Related Diseases. Front Immunol [Internet] 2021 [cited 2022 Dec 5];12. Available from: https://www.frontiersin.org/articles/10.3389/fimmu.2021.678918
26. Smith T Insights into the role of fibroblasts in human autoimmune diseases. Clin Exp Immunol 2005 Sep;141(3):388–97. [PubMed: 16045727]
27. Ganguly D, Haak S, Sisirak V, Reizis B. The role of dendritic cells in autoimmunity. Nat Rev Immunol 2013 Aug;13(8):566–77. [PubMed: 23827956]
28. Saha I, Jaiswal H, Mishra R, Nel HJ, Schreuder J, Kaushik M, et al. RelB suppresses type I Interferon signaling in dendritic cells. Cell Immunol 2020 Mar 1;349:104043. [PubMed: 32044112]
29. Ratra Y, Kumar N, Saha MK, Bharadwaj C, Chongtham C, Bais SS, et al. A Vitamin D–RelB/NF-κB Pathway Limits Chandipura Virus Multiplication by Rewiring the Homeostatic State of Autoregulatory Type 1 IFN–IRF7 Signaling. J Immunol [Internet] 2022 Jul 18 [cited 2022 Aug 18]; Available from: https://www.jimmunol.org/content/early/2022/07/18/jimmunol.2101054
30. Jin J, Hu H, Li HS, Yu J, Xiao Y, Brittain GC, et al. Noncanonical NF-κB Pathway Controls the Production of Type I Interferons in Antiviral Innate Immunity. Immunity 2014 Mar 20;40(3):342–54. [PubMed: 24656046]
31. Cheng CS, Behar MS, Suryawanshi GW, Feldman KE, Spreafico R, Hoffmann A. Iterative Modeling Reveals Evidence of Sequential Transcriptional Control Mechanisms. Cell Syst 2017 Mar;4(3):330–343.e5. [PubMed: 28237795]
32. Martin M Cutadapt removes adapter sequences from high-throughput sequencing reads. EMBnet.journal 2011 May 2;17(1):10–2.

33. Dobin A, Davis CA, Schlesinger F, Drenkow J, Zaleski C, Jha S, et al. STAR: ultrafast universal RNA-seq aligner. Bioinforma Oxf Engl 2013 Jan 1;29(1):15–21.
34. Twelve years of SAMtools and BCFtools | GigaScience | Oxford Academic [Internet] [cited 2022 Sep 29]. Available from: https://academic.oup.com/gigascience/article/10/2/giab008/6137722
35. Liao Y, Smyth GK, Shi W. featureCounts: an efficient general purpose program for assigning sequence reads to genomic features. Bioinforma Oxf Engl 2014 Apr 1;30(7):923–30.
36. Frankish A, Diekhans M, Ferreira AM, Johnson R, Jungreis I, Loveland J, et al. GENCODE reference annotation for the human and mouse genomes. Nucleic Acids Res 2019 Jan 8;47(D1):D766–73. [PubMed: 30357393]
37. Robinson MD, McCarthy DJ, Smyth GK. edgeR: a Bioconductor package for differential expression analysis of digital gene expression data. Bioinformatics 2010 Jan 1;26(1):139–40. [PubMed: 19910308]
38. Lutz MB, Kukutsch N, Ogilvie AL, Rössner S, Koch F, Romani N, et al. An advanced culture method for generating large quantities of highly pure dendritic cells from mouse bone marrow. J Immunol Methods 1999 Feb 1;223(1):77–92. [PubMed: 10037236]
39. Shih VFS, Davis-Turak J, Macal M, Huang JQ, Ponomarenko J, Kearns JD, et al. Control of RelB during dendritic cell activation integrates canonical and noncanonical NF-κB pathways. Nat Immunol 2012 Dec;13(12):1162–70. [PubMed: 23086447]
40. Sen S, Cheng Z, Sheu KM, Chen YH, Hoffmann A. Gene Regulatory Strategies that Decode the Duration of NFκB Dynamics Contribute to LPS- versus TNF-Specific Gene Expression. Cell Syst 2020 Feb;10(2):169–182.e5. [PubMed: 31972132]
41. Schneider WM, Chevillotte MD, Rice CM. Interferon-Stimulated Genes: A Complex Web of Host Defenses. Annu Rev Immunol 2014;32:513–45. [PubMed: 24555472]
42. Assouvie A, Daley-Bauer LP, Rousselet G. Growing Murine Bone Marrow-Derived Macrophages. In: Rousselet G, editor. Macrophages: Methods and Protocols [Internet] New York, NY: Springer; 2018 [cited 2022 Sep 21]. p. 29–33. (Methods in Molecular Biology). Available from: 10.1007/978-1-4939-7837-3_3
43. Blanco P, Palucka AK, Pascual V, Banchereau J. Dendritic cells and cytokines in human inflammatory and autoimmune diseases. Cytokine Growth Factor Rev 2008 Feb;19(1):41–52. [PubMed: 18258476]
44. Hilligan KL, Ronchese F. Antigen presentation by dendritic cells and their instruction of CD4+ T helper cell responses. Cell Mol Immunol 2020 Jun;17(6):587–99. [PubMed: 32433540]
45. Embgenbroich M, Burgdorf S. Current Concepts of Antigen Cross-Presentation. Front Immunol [Internet] 2018 [cited 2022 Sep 21];9. Available from: https://www.frontiersin.org/articles/10.3389/fimmu.2018.01643
46. Wang W, Xu L, Su J, Peppelenbosch MP, Pan Q. Transcriptional Regulation of Antiviral Interferon-Stimulated Genes. Trends Microbiol 2017 Jul;25(7):573–84. [PubMed: 28139375]
47. Cheng CS, Feldman KE, Lee J, Verma S, Huang DB, Huynh K, et al. The Specificity of Innate Immune Responses Is Enforced by Repression of Interferon Response Elements by NF-κB p50. Sci Signal 2011 Feb 22;4(161):ra11. [PubMed: 21343618]
48. Pfeffer LM, Kim JG, Pfeffer SR, Carrigan DJ, Baker DP, Wei L, et al. Role of Nuclear Factor-κB in the Antiviral Action of Interferon and Interferon-regulated Gene Expression*. J Biol Chem 2004 Jul 23;279(30):31304–11. [PubMed: 15131130]
49. Wei L, Sandbulte MR, Thomas PG, Webby RJ, Homayouni R, Pfeffer LM. NFκB NEGATIVELY REGULATES INTERFERON-INDUCED GENE EXPRESSION AND ANTI-INFLUENZA ACTIVITY. J Biol Chem 2006 Apr 28;281(17):11678–84. [PubMed: 16517601]
50. Fitzgerald KA, McWhirter SM, Faia KL, Rowe DC, Latz E, Golenbock DT, et al. IKKε and TBK1 are essential components of the IRF3 signaling pathway. Nat Immunol 2003 May;4(5):491–6. [PubMed: 12692549]
51. Parvatiyar K, Pindado J, Dev A, Aliyari SR, Zaver SA, Gerami H, et al. A TRAF3-NIK module differentially regulates DNA vs RNA pathways in innate immune signaling. Nat Commun 2018 Jul 17;9(1):2770. [PubMed: 30018345]

52. Barton D, HogenEsch H, Weih F. Mice lacking the transcription factor RelB develop T cell-dependent skin lesions similar to human atopic dermatitis. Eur J Immunol 2000;30(8):2323–32. [PubMed: 10940923]
53. Ashley CL, Abendroth A, McSharry BP, Slobedman B. Interferon-Independent Innate Responses to Cytomegalovirus. Front Immunol [Internet] 2019 [cited 2022 Dec 6];10. Available from: https://www.frontiersin.org/articles/10.3389/fimmu.2019.02751
54. Ashley CL, Abendroth A, McSharry BP, Slobedman B. Interferon-Independent Upregulation of Interferon-Stimulated Genes during Human Cytomegalovirus Infection is Dependent on IRF3 Expression. Viruses 2019 Mar 12;11(3):246. [PubMed: 30871003]
55. Rutherford HA, Kasher PR, Hamilton N. Dirty Fish Versus Squeaky Clean Mice: Dissecting Interspecies Differences Between Animal Models of Interferonopathy. Front Immunol [Internet] 2021 [cited 2022 Nov 23];11. Available from: https://www.frontiersin.org/articles/10.3389/fimmu.2020.623650
56. Zeng Z, Lan T, Wei Y, Wei X. CCL5/CCR5 axis in human diseases and related treatments. Genes Dis 2022 Jan 1;9(1):12–27. [PubMed: 34514075]
57. Lv D, Zhang Y, Kim HJ, Zhang L, Ma X. CCL5 as a potential immunotherapeutic target in triple-negative breast cancer. Cell Mol Immunol 2013 Jul;10(4):303–10. [PubMed: 23376885]
58. Castell-Rodríguez A, Piñón-Zárate G, Herrera-Enríquez M, Jarquín-Yáñez K, Medina-Solares I, Castell-Rodríguez A, et al. Dendritic Cells: Location, Function, and Clinical Implications [Internet]. Biology of Myelomonocytic Cells IntechOpen; 2017 [cited 2022 Nov 5]. Available from: https://www.intechopen.com/state.item.id
59. McAnulty RJ. Fibroblasts and myofibroblasts: Their source, function and role in disease. Int J Biochem Cell Biol 2007 Jan 1;39(4):666–71. [PubMed: 17196874]
60. Carenza C, Calcaterra F, Oriolo F, Di Vito C, Ubezio M, Della Porta MG, et al. Costimulatory Molecules and Immune Checkpoints Are Differentially Expressed on Different Subsets of Dendritic Cells. Front Immunol [Internet] 2019 [cited 2022 Nov 5];10. Available from: https://www.frontiersin.org/articles/10.3389/fimmu.2019.01325
61. Hubo M, Trinschek B, Kryczanowsky F, Tüttenberg A, Steinbrink K, Jonuleit H. Costimulatory Molecules on Immunogenic Versus Tolerogenic Human Dendritic Cells. Front Immunol [Internet] 2013 [cited 2022 Nov 5];4. Available from: https://www.frontiersin.org/articles/10.3389/fimmu.2013.00082
62. Weih F, Durham SK, Barton DS, Sha WC, Baltimore D, Bravo R. Both multiorgan inflammation and myeloid hyperplasia in RelB-deficient mice are T cell dependent. J Immunol Baltim Md 1950 1996 Nov 1;157(9):3974–9.
63. Hemmi H, Takeuchi O, Sato S, Yamamoto M, Kaisho T, Sanjo H, et al. The Roles of Two IκB Kinase-related Kinases in Lipopolysaccharide and Double Stranded RNA Signaling and Viral Infection. J Exp Med 2004 Jun 21;199(12):1641–50. [PubMed: 15210742]
64. Sanchez GAM, Reinhardt A, Ramsey S, Wittkowski H, Hashkes PJ, Berkun Y, et al. JAK1/2 inhibition with baricitinib in the treatment of autoinflammatory interferonopathies. J Clin Invest 2018 Jul 2;128(7):3041–52. [PubMed: 29649002]
65. Jaan A, Rajnik M. TORCH Complex. In: StatPearls [Internet] Treasure Island (FL): StatPearls Publishing; 2022 [cited 2022 Nov 6]. Available from: http://www.ncbi.nlm.nih.gov/books/NBK560528/
66. Rice GI, Melki I, Frémond ML, Briggs TA, Rodero MP, Kitabayashi N, et al. Assessment of Type I Interferon Signaling in Pediatric Inflammatory Disease. J Clin Immunol 2017 Feb 1;37(2):123–32. [PubMed: 27943079]
67. Morand EF, Furie R, Tanaka Y, Bruce IN, Askanase AD, Richez C, et al. Trial of Anifrolumab in Active Systemic Lupus Erythematosus. N Engl J Med 2020 Jan 16;382(3):211–21. [PubMed: 31851795]
68. Volpi S, Picco P, Caorsi R, Candotti F, Gattorno M. Type I interferonopathies in pediatric rheumatology. Pediatr Rheumatol 2016 Jun 4;14(1):35.
69. Baccala R, Gonzalez-Quintial R, Schreiber RD, Lawson BR, Kono DH, Theofilopoulos AN. Anti-IFNAR Antibody Treatment Ameliorates Disease in Lupus-Predisposed Mice. J Immunol Baltim Md 1950 2012 Dec 15;189(12):5976–84.

70. Zhou Q, Wang H, Schwartz DM, Stoffels M, Park YH, Zhang Y, et al. Loss-of-function mutations in TNFAIP3 leading to A20 haploinsufficiency cause an early-onset autoinflammatory disease. Nat Genet 2016 Jan;48(1):67–73. [PubMed: 26642243]

71. Aeschlimann FA, Batu ED, Canna SW, Go E, Gül A, Hoffmann P, et al. A20 haploinsufficiency (HA20): clinical phenotypes and disease course of patients with a newly recognised NF-kB-mediated autoinflammatory disease. Ann Rheum Dis 2018 May 1;77(5):728–35. [PubMed: 29317407]

72. Clarke SLN, Robertson L, Rice GI, Seabra L, Hilliard TN, Crow YJ, et al. Type 1 interferonopathy presenting as juvenile idiopathic arthritis with interstitial lung disease: report of a new phenotype. Pediatr Rheumatol 2020 May 12;18(1):37.

73. Kadowaki T, Ohnishi H, Kawamoto N, Hori T, Nishimura K, Kobayashi C, et al. Haploinsufficiency of A20 causes autoinflammatory and autoimmune disorders. J Allergy Clin Immunol 2018 Apr 1;141(4):1485–1488.e11. [PubMed: 29241730]

74. Gedik KC, Lamot L, Romano M, Demirkaya E, Piskin D, Torreggiani S, et al. The 2021 European Alliance of Associations for Rheumatology/American College of Rheumatology points to consider for diagnosis and management of autoinflammatory type I interferonopathies: CANDLE/PRAAS, SAVI and AGS. Ann Rheum Dis 2022 May 1;81(5):601–13. [PubMed: 35086813]

75. Paredes JL, Niewold TB. Type I interferon antagonists in clinical development for lupus. Expert Opin Investig Drugs 2020 Sep;29(9):1025–41.

Key Messages

- Human and mouse NFκB RelB deficiency leads to multi-organ auto-immune pathology.
- Unbiased profiling of patient derived fibroblasts reveals a broad interferon gene signature which is also present in RelB knockout mouse dendritic cells.
- Compound deficiency of the interferon type I receptor completely ablates this gene program, but does not diminish RelB knockout autoimmune pathology, ruling out interferonopathy.

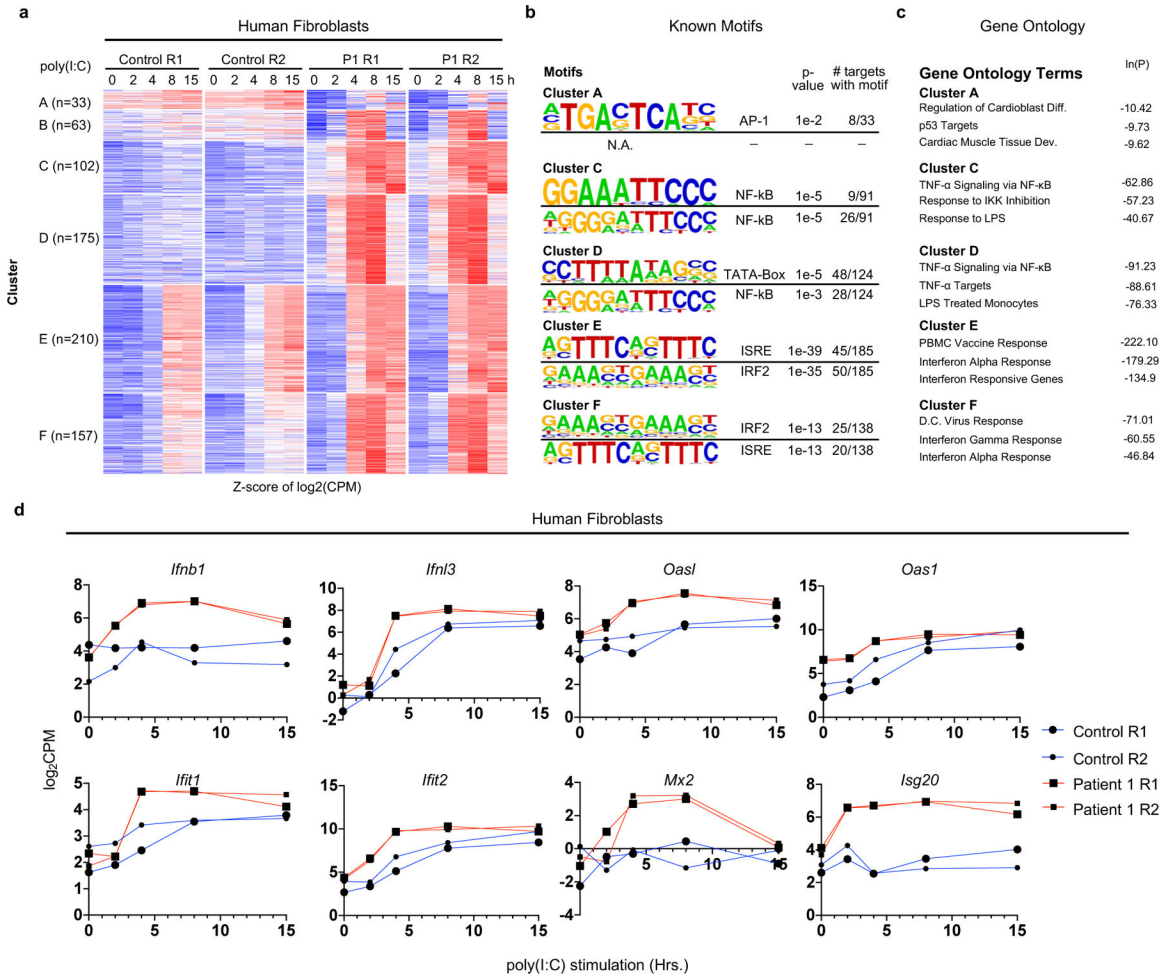

Fig. 1. Fibroblasts obtained from a human *RelB*-null donor show hyperexpression of type I interferon and interferon-stimulated genes.

a Heatmap of z-scored log_2CPM of all poly(I:C)(10μg/ml)-induced (FC>4 and FDR <0.01) genes in Control or P1 (RelB-null) derived fibroblasts (740 genes). Each row represents individual genes, and each column is from an individual time point post stimulation. R1 and R2 are experimental replicates. Red and blue colors represent distance from mean log_2CPM value for each gene. **b** Top two results of known motif analysis results for gene clusters from Fig. 1a. Motif analysis considered −4kb to +1kB with respect to the transcription start site (TSS). Cluster B did not generate motifs with given parameters. (N.A.=No motif result) **c** Gene ontology results for gene clusters from Fig. 1a. **d** Line graphs of gene expression (log_2CPM) for *Ifn*-β, and *Ifn*- λ3, and several ISGs during poly(I:C)-stimulation (0,2,4,8 and 15hr) (blue line represents control patient derived fibroblasts, Rep. 1= large circle, Rep.2= small circle, red line represents P1 patient derived fibroblasts, Rep. 1= large square, Rep.2= small square).

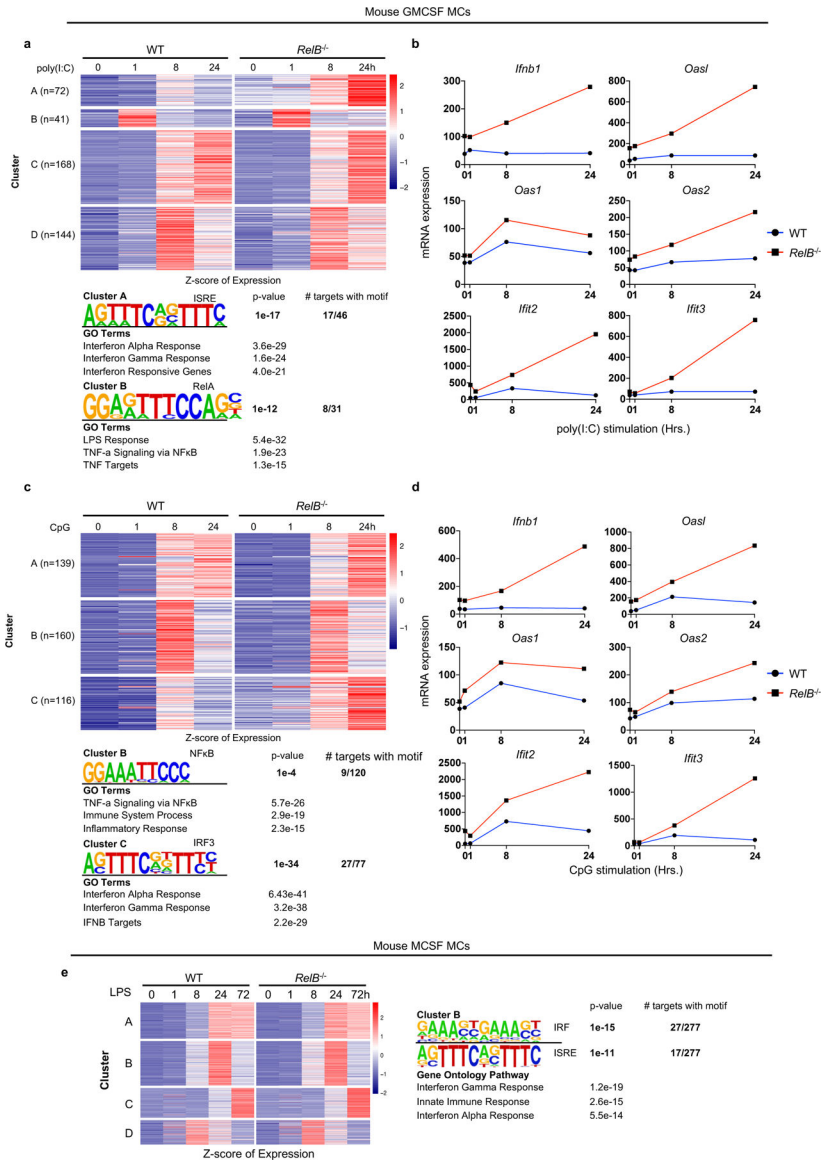

Fig. 2. Loss of RelB in mouse myeloid cells recapitulate hyperexpression of type I IFN and interferon stimulated gene programs.

a Heatmap of z-scored mRNA expression of all poly(I:C)-induced (10μg/ml) (logFC>1) genes in WT GMCSF MCs (425 genes) *(upper panel)*. Motif analysis and GO results for gene clusters from Fig. 2a *(lower panel)* **b** Line graphs of mRNA expression during poly(I:C)-stimulation (0,1,3,8 and 24hr), blue line (circle) represents WT GMCSF MCs, red line (square) represents *RelB*$^{-/-}$ GMCSF MCs **c (Top)** Heatmap of z-scored mRNA expression of all CPG-induced (0.1μM) (logFC>1) genes in WT MCs (415 genes). **c (Bottom)** Motif analysis and GO results for gene clusters from Fig. 2c **d** Line graphs of mRNA expression during CpG-stimulation (0,1,3,8 and 24hr), same color key as Fig 2b. **e (Left)** Heatmap of z-scored mRNA expression of all LPS-induced (logFC>1) genes in WT or *RelB*$^{-/-}$ MCSF MCs (1,243 unique genes). **e (Right)** Motif analysis and gene ontology results from gene cluster B of Fig. 2e. Each row in heatmaps represents individual genes, each column is an individual time point during stimulation. Motif analysis showing top

statistically significant motif analysis result (*known or de-novo*) considering −1kb to +1kB with respect to the TSS.

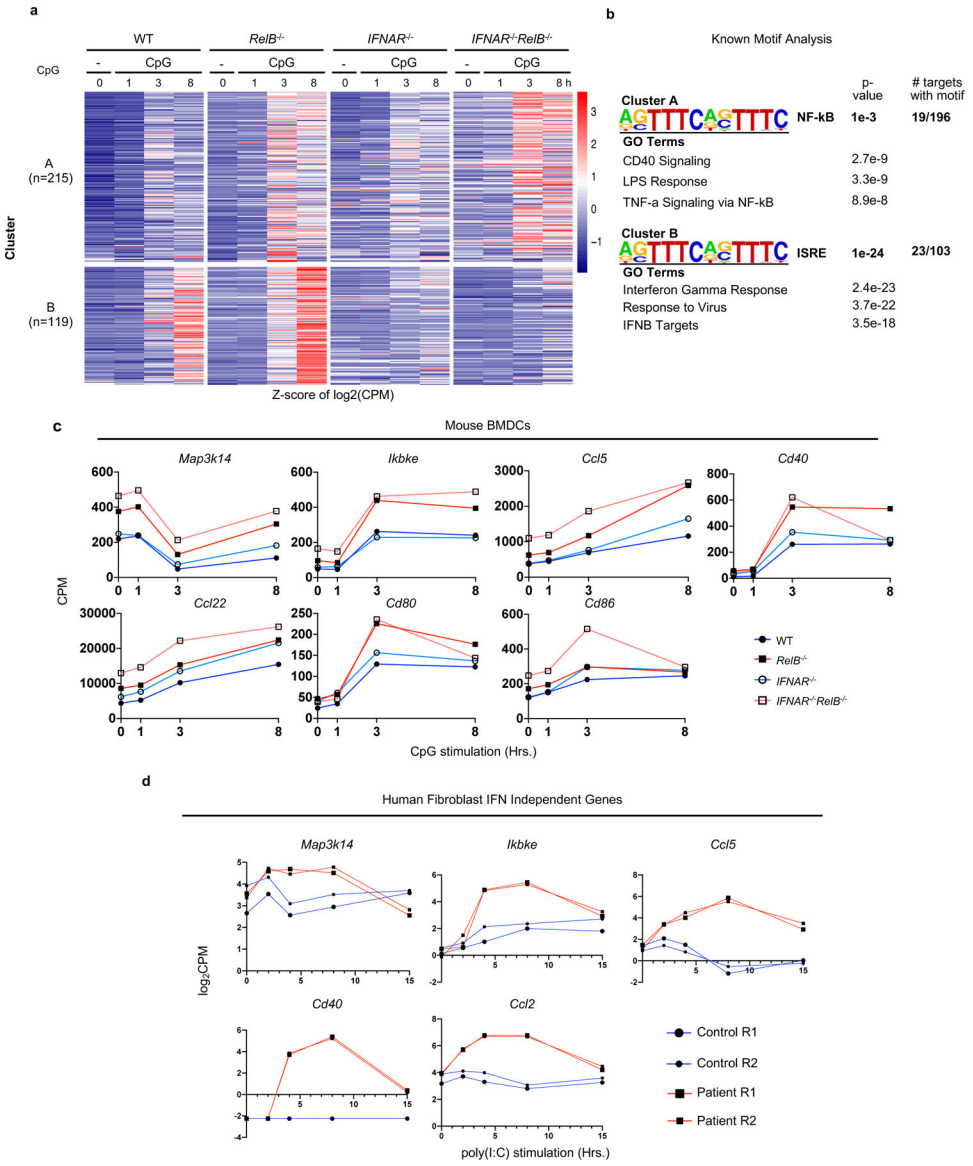

Fig. 3. Type I IFN receptor compound deficiency ablates the elevated IFN-stimulated gene program but reveals other immune response genes suppressed by RelB independent of type I IFN signaling.

a Heatmap of z-scored CPM of all *RelB*$^{-/-}$ hyper-expressed genes in WT, *RelB*$^{-/-}$, *IFNAR*$^{-/-}$, and *IFNAR*$^{-/-}$*RelB*$^{-/-}$ MCs. Genes selected for CpG-induced (0.1μM) (logFC>1) in WT or *RelB*$^{-/-}$ MCs & hyper-expressed (FC>1.5) in *RelB*$^{-/-}$ MCs relative to WT MCs at any time point (334 genes). Each row represents individual genes, each column is from an individual time point during stimulation. **b** Top known motif analysis and gene ontology results for gene clusters from Fig. 3a. **c** Line graphs of CPM for IFN-independent hyper-expressed genes from cluster A from Fig. 3a and genes with similar functions during CpG-stimulation (0,1,3, and 8hr), dark blue line (closed circle) represents WT GMCSF MCs, dark red line (closed square) represents *RelB*$^{-/-}$ GMCSF MCs, light blue line (open circle) represents *IFNAR*$^{-/-}$ GMCSF MCs, light red line (open square) represents *IFNAR*$^{-/-}$*RelB*$^{-/-}$ GMCSF MCs. **d** Line graphs of $\log_2$CPM for genes from

cluster A in Fig. 3a and genes with similar functions in patient derived fibroblasts from Fig. 1a. Poly(I:C)-stimulation (0,2,4,8 and 15hr), (blue line represents control patient derived fibroblasts, Rep. 1= large circle, Rep.2= small circle, red line represents P1 patient derived fibroblasts, Rep. 1= large square, Rep.2= small square). Motif analysis considered −1kb to +1kB with respect to the TSS.

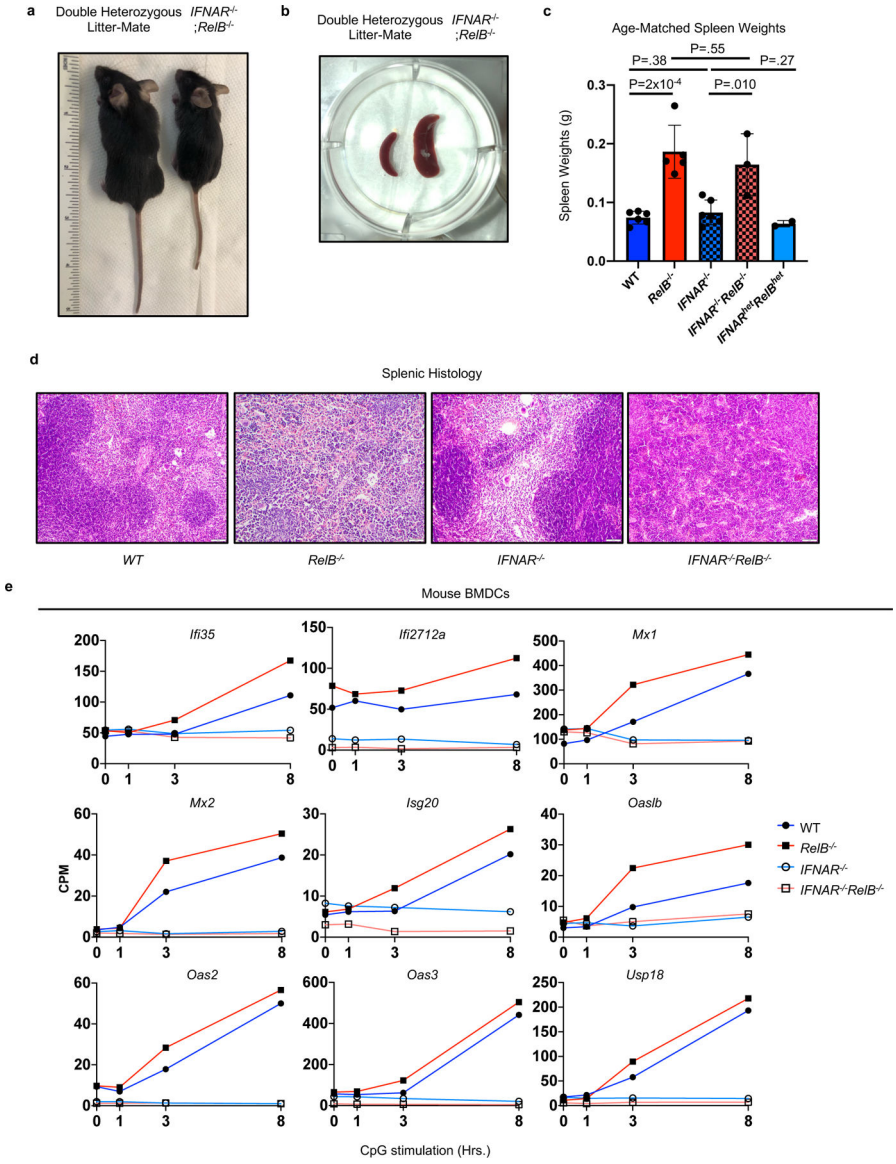

Fig. 4. Ablation of the elevated type I IFN-stimulated gene program does not rescue RelB-null pathology.

a Representative image of *IFNAR*$^{-/-}$*;RelB*$^{-/-}$ **(Right)** and healthy litter mate **(Left)** at 4 weeks of age, ruler for scale. **b** Representative image of spleens from *IFNAR*$^{-/-}$*;RelB*$^{-/-}$ mice **(Right)** and healthy litter mate **(Left) c** Spleen weights from age-matched WT (solid dark blue), *RelB*$^{-/-}$ (solid dark red), *IFNAR*$^{-/-}$(checkered light blue), *IFNAR*$^{-/-}$*RelB*$^{-/-}$ (checkered light red), and *IFNAR*^{het}*RelB*^{het} (solid light blue) mice. Error bars indicate S.D. Statistical analysis was done using unpaired 2-tailed students t-test **d** Representative images from histology of WT, *RelB*$^{-/-}$, *IFNAR*$^{-/-}$, and *IFNAR*$^{-/-}$*RelB*$^{-/-}$ spleens, demonstrating loss of white pulp and expansion of red pulp in *IFNAR*$^{-/-}$*RelB*$^{-/-}$ spleens. White bar for scale (bottom right, 50μm) **e** Line graphs of gene expression (CPM) for ISGs showing loss of induction in *IFNAR*$^{-/-}$ (light blue, open circle) and *IFNAR*$^{-/-}$*RelB*$^{-/-}$ (light red, open square) mice during CpG-stimulation (0,1,3, and 8hr). Dark blue line (closed circle) represents WT GMCSF MCs, dark red line (closed square) represents *RelB*$^{-/-}$ GMCSF

MCs, light blue line (open circle) represents *IFNAR*$^{-/-}$ GMCSF MCs, light red line (open square) represents *IFNAR*$^{-/-}$*RelB*$^{-/-}$ GMCSF MCs.